

**Isolation and Evaluation of Pharmacological Activities of a Bioactive Hydroxylated C28 Steroid from the Leaf of *Laportea decumana* (Roxb.) Wedd**

Rollando Rollando*, Eva Monica, Muhammad H. Aftoni, Christopher D. Kurniawan, Rehmadata Sitepu

Department of Pharmacy, Faculty of Science and Technology, Ma Chung University, Malang 65151, Indonesia

ARTICLE INFO

Article history:

Received 22 April 2022

Revised 29 June 2022

Accepted 25 July 2022

Published online 03 August 2022

Copyright: © 2022 Rollando *et al.* This is an open-access article distributed under the terms of the [Creative Commons Attribution License](https://creativecommons.org/licenses/by/4.0/), which permits unrestricted use, distribution, and reproduction in any medium, provided the original author and source are credited.

ABSTRACT

Cancer and infection rates have risen significantly in the last decade. Medicinal plants can be used to treat cancer and infections. *Laportea decumana* (Roxb.) Wedd for example, has long been used as a medicinal plant, but scientific evidence on its pharmacological effects is limited. The present study was therefore aimed at isolating a bioactive compound from the leaves of *Laportea decumana* and evaluating its pharmacological activities. Ethanol was used to extract the leaves of *L. decumana* using the maceration method. Preparative thin layer chromatography (TLC) was used for the isolation of an active compound, and preparative high-performance liquid chromatography (HPLC) was employed for purification. The structure of the active compound was determined by UV/Vis, IR, MS, ¹H-NMR, ¹³C-NMR, HMQC, and HMBC. *Staphylococcus aureus* and *Escherichia coli* were used to examine the antibacterial activity of the compound. Furthermore, the antioxidant potential of the new compound was determined by the DPPH (2,2-diphenyl-1-picrylhydrazyl) assay. Molecular docking was performed with the PyRx program. Also, the compound was tested for its ability to inhibit 4T1 cancer cells. The results showed that the extraction process yielded an oily green, thick extract with a yield value of 5.19%. From the leaves of *L. decumana*, a new hydroxylated C28 steroid was isolated (MCI). The bioactive compound possessed antibacterial properties against the test organisms, as well as antioxidant activity by DPPH assay. Furthermore, MCI was active against 4T1 cancer cells. The findings of this study suggest that MCI has the potential as a cancer cell inhibitor.

Keywords: Antibacterial, Antioxidant, Cytotoxic, *Laportea decumana*, Molecular docking.

Introduction

Laportea decumana (Roxb.) Wedd is a medicinal plant native to Indonesia. It is widely grown in Papua and Papua New Guinea and has been used as a herbal remedy to treat pain and headaches.¹ It has potential pharmacological activity due to the presence of alkaloid, glycoside, and triterpenoid contents.² Previous studies found that *L. decumana* extract has analgesic and antibacterial properties.³ The plant extract is a complex mixture of soluble compounds in the extractive solvent, including primary metabolites (molecular mass ≥ 2000 Dalton) and secondary metabolites (molecular mass < 2000 Dalton). Although secondary metabolites like alkaloid, flavonoid, coumarin, quinone, and terpenoid have important biological activities,⁴ the presence of primary metabolites in extracts make a quantitative determination of the active compound dose impossible. The research on *L. decumana* pharmacological activity was only reported as an extract form in the literature study, so the active compound was still unknown. Therefore, the present study was conducted to isolate a bioactive compound from the leaves of *Laportea decumana* and assess its pharmacological activities.

*Corresponding author. E mail: ro.llando@machung.ac.id
Tel: +6282220379864

Citation: Rollando R, Monica E, Aftoni MH, Kurniawan CD, Sitepu R. Isolation and Evaluation of Pharmacological Activities of a Bioactive Hydroxylated C28 Steroid from the Leaf of *Laportea decumana* (Roxb.) Wedd. Trop J Nat Prod Res. 2022; 6(7):1096-1102. doi.org/10.26538/tjnpr/v6i7.9

Official Journal of Natural Product Research Group, Faculty of Pharmacy, University of Benin, Benin City, Nigeria.

Materials and Methods

Sources of chemicals

Silica gel F₂₅₄, Silica gel 60 PF₂₅₄ containing gypsum, dimethyl sulfoxide (DMSO), methanol, chloroform, n-hexane, and ethyl acetate were obtained from Merck, United States. Dextrose, nutrient agar (NA), and Mueller Hinton were purchased from Oxoid, United Kingdom. RPMI 1640, fetal bovine serum, penicillin, streptomycin, fungizone, sodium bicarbonate, and L-glutamine were supplied by Gibco, United States. HEPES (4-[2-hydroxyethyl]-1-piperazineethanesulfonic acid) were purchased from Invitrogen, United States. DPPH (2,2-diphenyl-1-picrylhydrazyl) and MTT (3-[4,5-dimethylthiazol-2-yl]-2,5-diphenyltetrazolium bromide) were obtained from Sigma-Aldrich, United States.

Source of plant materials

The leaves of *Laportea decumana* were collected in January 2022 from Sorong, West Papua, Indonesia, and authenticated in the Department of Botany, University of Ma Chung, Indonesia. A voucher specimen number (FA:02-MACHUNG-2022) was assigned and the plant material was deposited in the herbarium unit of the department. Fresh leaves were washed and impurities were removed. The leaves were dried in an oven at 50°C for two days and then pulverized.⁵

Extraction of *Laportea decumana* leaves

The extraction was accomplished through maceration at room temperature by soaking 150 g dried leaf sample in 1 L 96% ethanol for 24 hours. The filtered mixture was collected. To obtain a thicker filtrate, the obtained filtrate was evaporated in a rotary evaporator, which was followed by advanced evaporation in a water bath.⁶

Isolation of active compounds from *Laportea decumana* leaf extract

Isolation of active compounds was divided into four stages: solvent optimization, bioautography, preparative thin layer chromatography (TLC), and purification with preparative high-performance liquid

chromatography (HPLC), as depicted in Figure 1. Both solvent optimization and preparative TLC were performed using silica gel 60 GF₂₅₄. Before using the plate, the TLC plate was activated by heating it at 115°C for 1 hour. The activated preparative TLC plate was then treated with a 20 mg/mL *L. decumana leaf extract*. The triterpenoid compound was then separated by elution with n-hexane and ethyl acetate (4:1). Finally, the fraction was purified using preparative HPLC with methanol as the mobile phase.

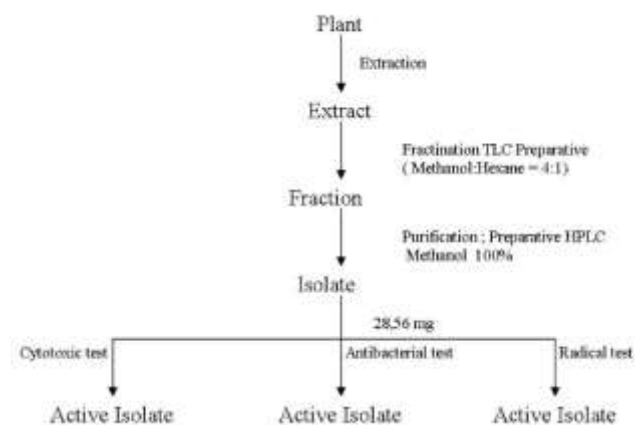


Figure 1: Schematic representation of active compound isolation

Antibacterial and antioxidant compound screening

The antibacterial compound screening was done by placing an eluted plate on an agar medium containing bacterial cells. The plate was left in contact with the agar surface for 3 hours before being removed. Then, the bacterial culture was incubated at 37°C for 24 hours. The position of an antibacterial compound on the TLC plate was indicated by a clear zone on the culture. Meanwhile, antioxidant compounds were screened by spraying a 25 µg/mL DPPH solution on an eluted TLC plate. After 30 minutes of incubation, a white band above the purple background indicated the presence of an antioxidant compound on the plate. Finally, the purity of the collected compound was determined using TLC and HPLC methods.⁷

Elucidation of the chemical structure of the isolated compound

The compound was determined using a qualitative reagent test and spectroscopy approaches by combining UV/Vis, IR, MS, ¹H-NMR, ¹³H-NMR, HMBC, and HMQC.

Determination of the antibacterial activity of the isolated compound

The antibacterial activity of the isolated compound was determined through minimal inhibitory concentration (MIC) and minimal bactericidal concentration (MBC) values. The MIC value was obtained by using a microdilution test. The test compound was prepared by dissolving the dried compound in a 2% DMSO solution. The microdilution test was performed by incubating a mixture of 50 µL broth medium, 50 µL bacterial culture with turbidity equivalent to 0.5 McFarland Standard, and 100 µL sample solution for 24 hours at 37°C. Negative control was made by replacing the sample with a liquid medium, while a positive control was prepared by substituting the sample with a 10 mg/mL streptomycin solution. After 24 hours of incubation, the clear solutions were streaked on an agar medium and incubated for another 24 hours. The lowest concentration that resulted in bacterial growth, indicated a MIC value, and the lowest concentration that resulted in no bacterial growth, indicated an MBC value.⁸

Evaluation of the antioxidant activity of the isolated compound

The compound containing 0.75, 1.5, 2.25, 3.0, or 6.0 µg/mL solution was made by dissolving the sample in methanol. In separate test tubes, 0.2 mL of each sample solution was mixed with 3.8 mL of 10 µg/mL DPPH solution. The solutions were incubated in a light-protected environment for 30 minutes, before being scanned with a UV/Vis

spectrophotometer at 517 nm. The antioxidant activity was determined using the following equation:⁹

$$\%Inhibition = \frac{A_{control} - A_{sample}}{A_{control}} \times 100$$

Where $A_{control}$ is the absorbance value of the control, and A_{sample} is the absorbance value of the sample.

Determination of the cytotoxic activity of the isolated compound

Using culture stock and culture medium, 4T1 cell culture was prepared at a concentration of 8,000 cells/well. The cell culture was transferred to a 96-well microplate and incubated for 24 hours in a 5% CO₂ incubator. After incubation, the cells in the wells were washed with PBS. The wells were then filled with 100 µL of each sample solution (1, 10, 25, 50, 75, 100, and 200 µg/mL) and incubated for 24 hours. After 24 hours, the cells were washed with PBS and a 100 µL MTT reagent was added to each well. Following 4 hours of incubation, 100 µL of stopper reagent (10% sodium dodecyl sulfate in 0.01 N HCl) was added and incubated for 24 hours in the dark. The number of viable cells was determined with an ELISA-reader at λ 595 nm.¹⁰ The percentage of cell growth inhibition, or percentage cytotoxicity, was calculated using the following formula:

$$\% Growth inhibition = 100 - \frac{\text{Mean OD of individual Test Group}}{\text{Mean OD of control Group}} \times 100$$

Cell cycle modulation on 4T1 cells

In 6 well plates, 1 mL of 5x10⁵ cells/well 4T1 culture was transferred. Every well received 900 µL of sample solution, which was then incubated for 24 hours. After the cells had been incubated, 1.5 ml of medium was transferred from the well to the conical tube. The remaining cells in the well were washed using 500 µL PBS. The PBS solution was then transferred to the conical tube. The remaining cells were collected using 200 µL of 0.25% trypsin-EDTA solution. Then, 1 ml of culture medium was added to each conical tube, and the tubes were centrifuged at 2000 rpm for 5 minutes to remove the PBS, leaving the cell beneath the tube. Flow cytometry reagent containing propidium iodide, Triton-X, and RNase was added to the prepared cells to observe the cell cycle. Meanwhile, an apoptotic induction test was performed on the prepared cells by adding a buffer kit annexin V-FLOUS reagent. After 10 minutes of incubation, the samples were analyzed with the flow cytometer FACS Calibur.¹¹

Molecular docking

The obtained chemical structure was converted to its 3D structure using the Chem3D Ultra program and saved as a *.pdb file. The PyMOL program was used to add hydrogen atoms and double bonds to the structure. The 3D structure was then uploaded to PyRx program to measure its partial energy and determine its best stereochemistry. The optimized structure was docked on several proteins downloaded from <http://www.rcsb.org/pdb/> by using Autodock Vina to determine their affinity value. Valid results were shown as interactions with an RMSD value of less than 2.0 and were saved as a *.pdb file to be visualized in the PyMOL program. The observation of interacting amino acid residues was done using the LigPlot program.¹²

Statistical analysis

The results were expressed as mean ± standard deviation of mean (SD).

Results and Discussion

Extraction yield and isolated compounds from the leaves of *Laportea decumana*

The extraction process produced an oily green thick extract with a yield value of 5.19%. Although the extraction by maceration method has low efficiency, it is safe for thermolabile products. Optimization, particularly in extraction method selection and extraction time, can increase yield value. The isolation of active compounds with the TLC method using n-hexane-ethyl acetate (4:1) produced optimal

separation on the plate. The weight of the isolate was 28.56 mg. Ten bands were identified under visible and UV₃₆₆, as shown in Table 1.

Table 1: R_f values of thin layer chromatography (TLC) plate

Sample	R _f value	Detector
Fraction 1	0.225	Visible, UV366
Fraction 2	0.3125	Visible, UV366
Fraction 3	0.3875	UV366
Fraction 4	0.4375	UV366
Fraction 5	0.5625	UV366
Fraction 6	0.625	Visible, UV366
Fraction 7	0.6875	UV366
Fraction 8	0.75	UV366
Fraction 9	0.875	UV366
Fraction 10	0.9375	Visible

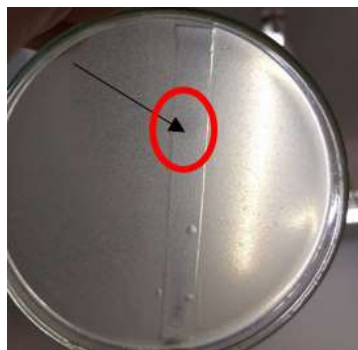


Figure 1: Bioautography result on *Staphylococcus aureus*.

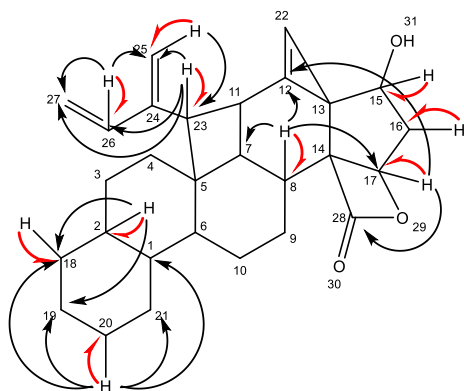


Figure 2: Structure of the bioactive compound. HMBC arrow () dan HMQC arrow () on MCI



Figure 3: Result of antibacterial test of MCI.

Antibacterial and antioxidant compound screened from the isolate

The antibacterial screening on *Staphylococcus aureus* and *Escherichia coli* was done using bioautography, which revealed antibacterial activity on *S. aureus* but no activity on *E. coli*. Figure 1 shows the antibacterial compound discovered on the fraction with an R_f value of 0.6875. The ability of the substance to diffuse from the plate into the agar medium determines the bioautography results. The non-polar terpenoid substance, on the other hand, prevents it from being absorbed into the medium. As a result, some active compounds may have gone undetected due to the low concentration of the compound in the agar medium. The screening of antioxidant compounds with 0.2 µg/mL DPPH solution revealed that the fraction with an R_f value of 0.6725 had free radical scavenging activity. The test result was blurry because a good observable result required an adequate amount of reagent and reactant. Despite the low concentration of the antioxidant compound adsorbed on the silica gel, the white band above the purple background could still be identified.

The isolated active compound by preparative thin layer chromatography

The weights of the dried fractions showed yield values of 38% for fraction 1, 2% for fraction 2, 2% for fraction 3, 1% for fraction 4, 4.4% for fraction 5, 10% for fraction 6, 3% for fraction 7, and 13% for fraction 8. The purity test was done only to fraction seven since the active compound screening showed only fraction seven to be active. The purity test of the TLC method reveals a single spot after elution with n-hexane-ethyl acetate (4:1), whereas the HPLC chromatogram revealed two peaks at retention times of 2.36 and 4.69 minutes. The AUC of the 2.36-minute peak was very low (5%), indicating that the peak could be caused by an impurity that will not interfere with the following test. The chemical structure of the 4.69-minute peak was identified.

Chemical structure of the isolated bioactive compound

The UV/Vis spectrum of fraction 7 showed a single peak at 266 nm, indicating that the compound contains a short chromophore chain. An absorbance at that wavelength indicated that the compound could contain a chromophore with two or three bonds. Meanwhile, the IR spectrum indicated that the compound has a hydroxyl group (3454.4 cm⁻¹), carbonyl or olefinic group (1658.87 cm⁻¹), and a lactone group (1262.66; 1232.60; and 1115.10 cm⁻¹). Other peaks on the IR spectrum showed that the compound is composed of alkane groups.¹³ The compound has 28 carbons, according to the ¹³C-NMR spectrum. Six olefinic atoms (C12, C22, C24, C25, C26, and C27) were detected in the chemical shift between 109.14 and 174.45 µg/mL. The carbon in 174.45 is responsible for the lactone group. Several carbon atoms were identified as the neighbours of the olefinic carbon or electronegative group for having a chemical shift of 63.61 (C11), 63.70 (C15), and 71.89 (C17) µg/mL. The DEPT spectrum showed no methyl (-CH₃) group, indicating that the compound is a heterocyclic molecule.

The ¹H-NMR spectrum exhibited several peaks with complex multiplicities. The two highest peaks were found at 1.04 and 2.36 µg/mL as doublets. A doublet was detected at 4.95 µg/mL, responsible for the six hydrogen atoms attached to the heteroatom environment. Those hydrogens were attached to a carbon atom near an oxygen atom or olefinic carbon (C15, C17, C26, C27). A single peak was also discovered at 6.62 µg/mL, which could be caused by a hydrogen atom attached to olefinic carbon (C25). The mass spectrum of the active compound identified the parental ion [M⁺H]⁺ with an m/z value of 419.61. Fragmentation of the compound shows three ions having an m/z value of 239.32, 261.32, and 441.62. The fragments with m/z values of 261.32 and 441.62 were obtained from fragments bonded to sodium atoms. Because no fragments indicated dimers, the molecular weight of the compound could be 418.61 g/mol. The 2D-NMR spectrums, which included HMQC and HMBC, were used as complementary data to interpret the chemical structure, which revealed a correlation (Table 2). The spectroscopy scanning data were combined to form the structure known as 9-(buta-1,3-dien-2-yl)-11-hydroxy-2,2a,2b,3,4,5,6,6a,7,8,8a,9,9a,12,12a,14b-hexadecahydro-1H,11H,14H-13-oxacyclobuta[1,5]-11-hydroxy-2,2a,2b,3,4,5,6,6a,7,8,8a,9,9a,12,12a,14b-hexacyclopenta[1,2-a]

cyclobuta[de] cyclopropa [b] chrysen-14-one, and was subsequently referred to as MC1. Thus, from the leaves of *L. decumana*, a new hydroxylated C28 steroid was isolated and identified. Figure 2 depicts the chemical structure as well as the correlation map.

Antibacterial activity of MC1

The antibacterial test on *S. aureus* revealed a MIC of 1600 µg/mL and an MBC of over 2000 µg/mL (Figure 3). Based on this result, it can be inferred that MC1 has weak antibacterial activity against *S. aureus* despite having a MIC value greater than 100 ppm. Meanwhile, previous research on *L. decumana* revealed that its extract had antibacterial activity against *S. aureus* and *E. coli*.¹⁴ However, the extract is a mixture of several compounds that create a synergic effect between constituent compounds, whereas MC1 as a single compound may have lower activity and thus lose the synergic effect. The mechanism by which MC1, as a steroid compound, demonstrated antibacterial activity was possibly due to a change in cell membrane function. Another antibacterial activity mechanism is that binding to elongation factor G (EF-G) inhibits protein synthesis, preventing polypeptide translocation.¹⁵ Chemical structure analysis revealed that the β-lactone group on the structure is similar to the β-lactam group, allowing it to interact with penicillin-binding proteins (PBP).¹⁶ Even though the *in vitro* test revealed weak antibacterial activity, this could be due to a high log P value (log P = 4) resulting in low water solubility. The compound's low solubility prevents it from penetrating the cell wall, resulting in weak activity.

Antioxidant activity of MC1

The antioxidant test on MC1 revealed an IC₅₀ value of 3.33±1.5 mg/mL, classifying it as a weak antioxidant because it had an IC₅₀ value greater than 150 µg/mL.¹⁷ The free radical scavenging activity of DPPH was used to determine antioxidant activity.

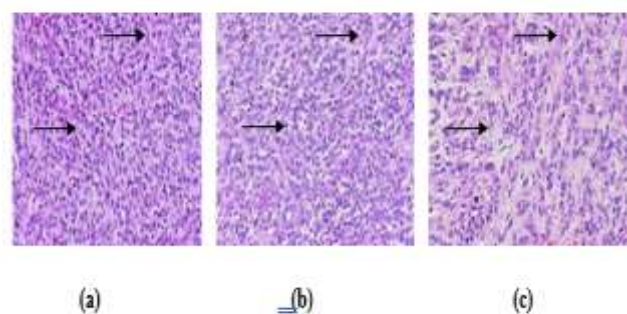


Figure 4: Cytotoxic effect of MC1 on 4T1 cancer cells. Morphological alteration after application of (a) Medium (-); (b) MC1 (71.77 µM); and (c) Doxorubicin (300 µM)

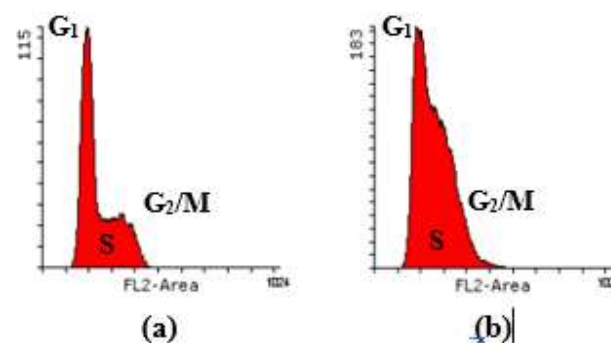


Figure 5: Cell cycle modulation of MC1 on 4T1 cells. (a) Negative control and (b) MC1 effect

Table 2: Correlation table of 2D-NMR

Hydrogen chemical shift (µg/mL)	HMQC (ppm)	HMBC (ppm)
1.07	C20 (23.53)	C19 (23.46), C18 (30.91), C21 (34.31), C1 (41.76)
2.29	C8 (39.12)	C7 (49.88), C12 (129.83), C17 (63.70)
	C23 (42.93)	C25 (124.97), C26(109.84), C27 (133.93)
2.36	C2 (42.10)	C18 (34.97), C19 (23.43)
2.86	C18 (34.97)	-
3.27	C16 (42.72)	-
4.27	C17 (63.70)	C12 (129.84), C28 (174.31)
4.60	C15 (71.83)	-
5.06	C26 (109.12)	C25 (124.97), C27 (133.93)
6.62	C25 (124.97)	C23 (42.93)
7.23	-	-

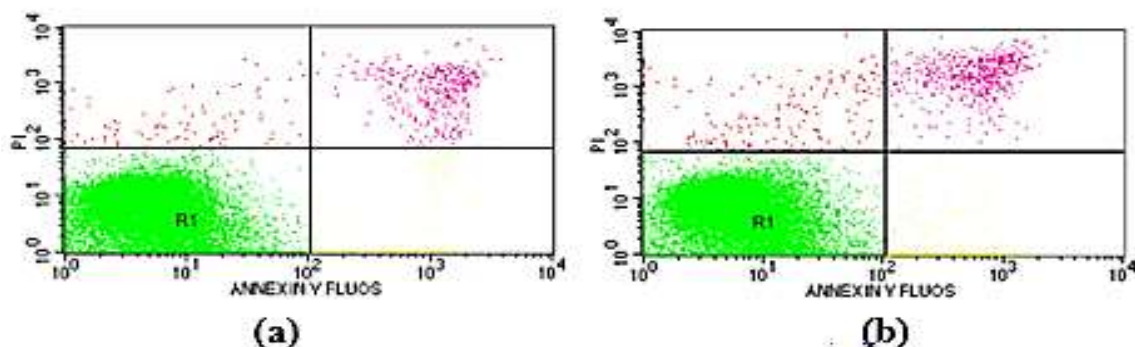


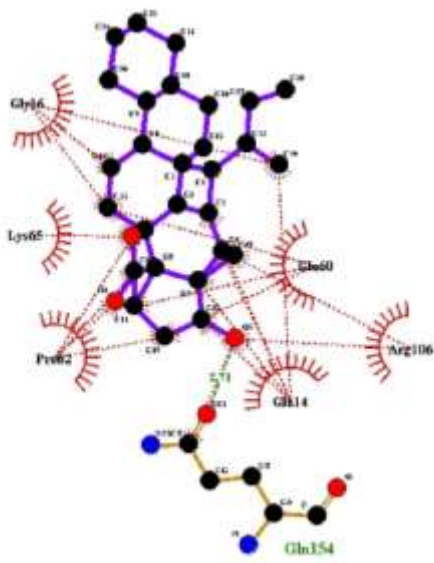
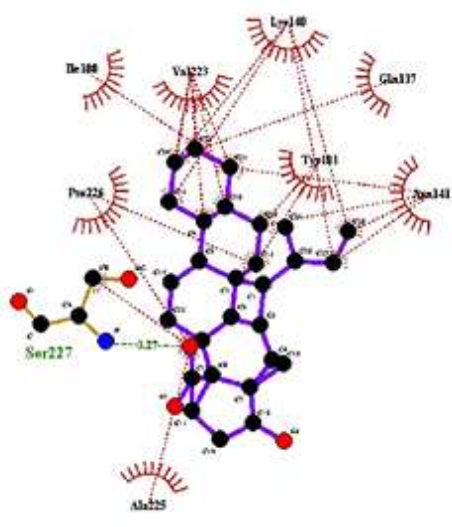
Figure 6: Flow cytometry result of MC1 on apoptotic induction test. (a) Negative control and (b) MC1 (71.77µM).

Table 3: Cell cycle distribution

Sample	G ₁ Phase (%)	S Phase (%)	G ₂ /M Phase (%)	% CV
Negative Control	49.39±0.23	10.35±0.32	23.07±0.25	9.08±0.21
MCI (71.77 µM)	27.46±0.37	27.70±0.11	16.30±0.63	7.85±0.39

Table 4: Percentage of cell death by different mechanisms

Mechanism	Negative control	MCI (71.77 µM)
Early apoptosis (%)	1.10±0.09	2.84±0.32
Late apoptosis (%)	1.85±0.03	2.90±0.22
Necrosis (%)	0.48±0.02	0.85±0.13
Total (%)	3.43±0.12	6.59±0.21

**Figure 7:** Interaction of MCI in PEX9**Figure 8:** Interaction of MCI in PGT

The reaction between the sample and DPPH was a second-order reaction, which means that the chemical structure of the reactant

influences the reaction rate.¹⁸ The weak antioxidant activity could be attributed to the rigid structure containing a trace amount of hydrogen and an electron donor group. The IC₅₀ value only represents the antioxidant activity on DPPH. It is still possible that MCI functions effectively as an antioxidant via another mechanism, such as chelate formation or an enzymatic mechanism, by inhibiting protein activity.¹⁹

Cytotoxic activity of MCI against 4T1 cancer cells

Cytotoxic activity testing on 4T1 breast cancer cells, a metastatic cancer cell, revealed promising activity with an IC₅₀ value of 33.31±1.59 µg/mL, or 71.77 µM. Figure 4 depicts the morphological change caused by the application of MCI to 4T1 cells. Morphological alterations were identified as reduced cell density and the formation of smaller fragments. These observations demonstrated cell death, but they did not describe the mechanism by which the cells died.²⁰ Even though MCI has a low cytotoxic activity (IC₅₀ > 10 µM),²¹ its IC₅₀ is still less than 100 M, implying that by modifying its side chain, it can be developed into a potent cytotoxic agent.¹¹

Cell cycle modulation of MCI on 4T1 cells

The 4T1 cells proliferate to increase in number. Cells typically accumulate at G₀/G₁ phase because p21 and p27 protein expression inhibit cyclin D activity, preventing it from proliferating.²² Meanwhile, the proliferation of cancer cells is threatening since mutations on the regulator gene prevent it from stopping even when damaged.²³ Therefore, the high proliferation rate was identified as a high number of cells distributed in the S phase and G₂ phase, as shown in Figure 5. The application of MCI on 4T1 cells caused an increase in the S phase and a decrease in other phases (Figure 5). Table 3 shows that the tested cells were distributed in S phase 17.35% higher than the control cell. As a result, the high proliferation rate was identified as a large number of cells distributed in the S and G₂ phases, as illustrated in Figure 5. When MCI was applied to 4T1 cells, it increased the S phase while decreasing the other phases. As shown in Table 3, the test cells were distributed in S phase, 17.35% higher than the control cells. The accumulation of cells in the S phase was possibly due to DNA damage or replication stress, which rendered the replication fork unable to perform DNA replication. It would cause a S phase arrest, preventing the cell from entering the G₂/M phase.²⁴ Furthermore, lactone terpenoid compound could decrease the expression of Cdc2, Cdk2, and Cyclin B1, which played a role as G₂ phase regulators. The decrease in their expression kept the cells in the S phase by preventing them from entering the G₂ phase.²⁵

Apoptosis induction of MCI on 4T1 cancer cells

Figure 6 depicts the apoptosis induction test on 4T1 cells, which shows an increase in the number of cell deaths after an application on 4T1. Table 4 shows that when compared to the negative control, the number of cell deaths due to apoptosis and necrosis was doubled. It demonstrated that MCI can cause 4T1 cell death, primarily via the apoptotic pathway. Because the 4T1 cancer cell was cultured with a p53 deficiency, apoptosis should occur via a p53-independent mechanism.²⁶ Alternatively, the therapy target for 4T1 cells can be pro-apoptotic gene stimulation, such as Bax, or inhibition of the protein that promotes metastasis. MMP9 protease was found to be upregulated in 4T1 cells. The enzyme is required for angiogenesis, making it a potential alternative target for suppressing 4T1 cells.²⁷

Molecular docking of MCI on hemopexin PEX9

Matrix metalloproteinase 9 is a zinc-dependent peptidase that can degrade collagen type IV on the basal lamina, providing a pathway for cell invasion. Before it can be activated, pro-MMP9 must bind to integrin on the surface of the tumor cell. Their attachment occurs at the non-catalytic domain, PEX9.²⁸ The molecular docking of MCI on

PEX9, especially on the sulfate ion binding pocket, showed an excellent interaction where both compounds interacted with Arg106. Furthermore, the binding affinity of the MC1 was -5.9 kcal/mol with an RMSD value of 1.733 Å, which is greater than the binding affinity of the sulfate ion (-3.5 kcal/mol). According to this information, MC1 could be a potential MMP9 inhibitor that works indirectly via the PEX9 domain (Figure 7).

Molecular docking of MC1 on peptidoglycan glycosyltransferase

The peptidoglycan chain, which is formed during the biosynthetic process, is the primary component of the bacterial cell wall. Peptidoglycan glycosyltransferase (PGT) is the enzyme that catalyzes this process. An inhibitor attached to PGT can prevent the glycan from annealing to the cell membrane. As a result, the inhibition causes a distraction to cell wall integrity.²⁹ Meanwhile, moenomycin is a well-known native PGT inhibitor. The docking of MC1 on PGT, particularly the moenomycin binding pocket, revealed an excellent interaction in which both compounds interacted with Val223, Lys140, Gln137, Ser227, Pro226, Asn141, Tyr181, and Ala225. Furthermore, the binding affinity of MC1 was -6.5 kcal/mol with an RMSD value of 0.368, which was less than moenomycin's binding affinity (-7.4 kcal/mol). This data confirms that MC1 can interact with PGT, but side chain modification will be required to improve its binding affinity to PGT as illustrated in Figure 8.

Conclusion

The present study discovered that *Laportea decumana* leaves contain an active compound known as 9-(buta-1,3-dien-2-yl)-11-hydroxy-2,2a,2b,3,4,5,6,6a,7,8,8a1,9,9a,12,12a,14b-hexadecahydro-1H,11H,14H-13-oxacyclobuta [1,5] cyclopenta [1,2-a]cyclobuta[de]cyclopropa[b]chrysen-14-one (MC1). The compound has antibacterial activity against *S. aureus*, free radical scavenging activity, and cytotoxic activity on 4T1 breast cancer cells. MC1 has great potential as a cancer cell inhibitor.

Conflict of Interest

The authors declare no conflict of interest.

Authors' Declaration

The authors hereby declare that the work presented in this article is original and that any liability for claims relating to the content of this article will be borne by them.

Acknowledgements

The authors would like to thank the Ministry of Education, Culture, Research, and Technology of the Republic of Indonesia for funding through "Penelitian Dasar Unggulan Perguruan Tinggi 2022" No. 045/SP2H/PT/LL7/2022.

References

1. Thalib A, Masadah R, Prihartono P, Hamid F, Hasan H, Keliwawa S, Labulawa I. *Laportea decumana* (roxb) wedd. herbal endemic potential from indonesia: a literature review. Open Access Maced. J Med Sci. 2021; 9(2):639–643.
2. Thalib A, Masadah R, Prihartono P, Hamid F, Hasan H, Keliwawa S, Labulawa I. Antioxidant activity of *Laportea decumana* (Roxb) Wedd ethanol and n-hexane extracts. Open Access Maced. J Med Sci. 2022; 10(2):590–594.
3. Simaremare ES, Putri CD, Pratiwi RD, Gunawan E. Itchy leaves (*Laportea decumana* (Roxb.) Wedd) simplicia loose powder. Malays. J Med Res. 2022; 6(2):9–13.
4. Gonçalves ECD. Terpenoids, cannabimimetic ligands, beyond the cannabis plant. Molecules. 2020; 25(4):156.
5. Lam DT. Two new terpenoids from the leaves of *Callicarpa macrophylla*. Nat Prod Res. 2021; 35(3):1107–1114.
6. Yuan FY. Three new terpenoids from *Chonemorpha megacalyx*. Nat Prod Res. 2022; 36(4):714–718.
7. Sun ZL, Liu T, Wang SY, Ji XY, Mu Q. TLC-bioautography directed isolation of antibacterial compounds from active fractionation of *Ferula feruloides*. Nat Prod Res. 2019; 33(9):1761–1764.
8. Astuti P, Rollando R, Wahyuono S, Nurrochmad A. Antimicrobial activities of isoprene compounds produced by an endophytic fungus isolated from the leaves of *Coleus amboinicus* Lour. J Pharm Pharmacogn Res. 2020; 8(4):280–289.
9. Hariono M and Rollando R. Bioguided fractionation of local plants against matrix metalloproteinase9 and its cytotoxicity against breast cancer cell models: *in silico* and *in vitro* study. Molecules.2020; 20(3):469.
10. Rollando R. Combination of *Hedyotis corymbosa* l. and *Tinospora crispa* ethanolic extract increase cisplatin cytotoxicity on T47D breast cancer cells. Asian J Pharm Clin Res. 2018; 3(3):171–177.
11. Rollando R, Warsito W, Masruri M, Widodo W. *Pterygota alata* (Roxb.) r.br. bark fraction induced intrinsic apoptotic pathway in 4T1 cells by decreasing bcl-2 and inducing bax expression. Pak J Biol Sci. 2021; 24(3):172–181.
12. Hariono M and Rollando, R. Arylamide as potential selective inhibitor for matrix metalloproteinase 9 (mmp9): design, synthesis, biological evaluation, and molecular modeling. J Chem Inf Model. 2020; 60(2): 349–359.
13. Kim CS, Oh J, Lee TH. Structure elucidation of small organic molecules by contemporary computational chemistry methods. Arch Pharm Res. 2020; 43(5):1114–1127.
14. Hariono M and Rolland R. Bioguided fractionation of local plants against matrix metalloproteinase9 and its cytotoxicity against breast cancer cell models: *in silico* and *in vitro* study (part II). Molecules. 2021; 26(4): 1464.
15. Rodnina MV, Peske F, Peng BZ, Belardinelli R, Wintermeyer W. Converting GTP hydrolysis into motion: versatile translational elongation factor G. Biol Chem. 2019; 401(5): 131–142.
16. Lima LM, Silva BNM, da Barbosa G, Barreiro EJ. β -lactam antibiotics: An overview from a medicinal chemistry perspective. Eur J Med Chem. 2019; 208(4):112829.
17. Mirzadeh M, Arianejad MR, Khedmat L. Antioxidant, antiradical, and antimicrobial activities of polysaccharides obtained by microwave-assisted extraction method: A review. Carbohydr Polym. 2020; 229(5):115421.
18. Sirivibulkovit K, Nouanthavong S, Sameenoi Y. Paper-based DPPH assay for antioxidant activity analysis. Annal Sci.2018; 34(2): 795–800.
19. Baschieri A and Amorati R. Methods to determine chain-breaking antioxidant activity of nanomaterials beyond DPPH•. A Review. Antioxidants. 2021; 10(3):1551.
20. Rollando R, Warsito W, Masruri M, Widodo W. *Sterculia foetida* leaf fraction against matrix metalloproteinase-9 protein and 4T1 breast cancer cells: in-vitro and in-silico studies. Trop J Nat Prod Res. 2021; 5(1): 113–121.
21. Rollando R and Prilianti KR. *Sterculia quadrifida* r.br ethyl acetate fraction increases cisplatin cytotoxicity on T47D breast cancer cells. Int J Pharm Res. 2018; 10(4): 204–212.
22. Wang J. CDK4/6 inhibitor-SHR6390 exerts potent antitumor activity in esophageal squamous cell carcinoma by inhibiting phosphorylated Rb and inducing G1 cell cycle arrest. J Transl Med. 2017; 15 (3):127.
23. Pecorino L. Molecular biology of cancer: mechanisms, targets, and therapeutics. Oxford. 2021; 3(6):123-135.
24. Zhao X, Zhang SS, Zhang XK, He F, Duan CQ. An effective method for the semi-preparative isolation of high-purity anthocyanin monomers from grape pomace. Food Chem. 2020; 310(4):125830.
25. Azevedo-Barbosa H. Phenylpropanoid-based sulfonamide promotes cyclin D1 and cyclin E down-regulation and

- induces cell cycle arrest at G1/S transition in estrogen positive MCF-7 cell line. *Tox Vit.* 2019; 59(4):150–160.
26. Steenbrugge J. Comparative profiling of metastatic 4T1- vs. non-metastatic py230-based mammary tumors in an intraductal model for triple-negative breast cancer. *Front Immunol.* 2019; 10(3):2928.
 27. Hariono M, Yuliani SH, Istyastono EP, Riswanto FDO, Adhipandito CF. Matrix metalloproteinase 9 (MMP9) in wound healing of diabetic foot ulcer: Molecular target and structure-based drug design. *Wound Med.* 2018; 22(3):1–13.
 28. Ugarte-Berzal E. A 17-residue sequence from the matrix metalloproteinase-9 (MMP-9) hemopexin domain binds $\alpha 4\beta 1$ integrin and inhibits MMP-9-induced functions in chronic lymphocytic leukemia B cells. *J Biol Chem.* 2012; 287(4):27601–27613.
 29. Mesleh MF. Targeting bacterial cell wall peptidoglycan synthesis by inhibition of glycosyltransferase activity. *Chem Biol Drug Des.* 2016; 87(4):190–199.